Physics Letters A 159 (1991) 390–395
North-Holland

PHYSICS LETTERS A

Dynamics of breather modes in a nonlinear "helicoidal" model of DNA

Thierry Dauxois

Physique Non-Linéaire: Ondes et Structures Cohérentes, Faculté des Sciences, Université de Bourgogne, 6 Boulevard Gabriel, 21000 Dijon, France

Received 25 April 1991; revised manuscript received 19 August 1991; accepted for publication 21 August 1991
Communicated by A.R. Bishop

We describe the dynamics of breather modes in DNA in terms of a recent lattice model with an additional interaction in order to take into account the helicoidal structure of the molecule. It is shown that, despite its simplicity, this model exhibits breatherlike modes which can match experimentally observed bubbles propagating along the helix. Numerical simulations of their propagation show these excitations to be long-lived and suggest that they are physically relevant for DNA.

1. Introduction

Biological macromolecules undergo a complex dynamics and the knowledge of their motions provides insight into biological phenomena [1]. Recently, attention has been focused on the dynamics of large-amplitude localized excitations in DNA [2–6], in which the double helix fluctuates between an open state and its equilibrium structure. These oscillatory states, also called breathing modes [7] or fluctuational openings, are expected to be the precursor states for the local denaturation observed during DNA transcription or thermal denaturation. In these studies, the molecule is modeled by two parallel chains of nucleotides, linked by nearest-neighbor harmonic interactions along the chains and the strands are coupled to each other by Morse potentials which represent the bonding inside one base pair. Such a model does not include the helical geometry of the molecule.

But one of the consequences of the helical structure is that nucleotides which are far apart in the one-dimensional model can be close enough in the three-dimensional structure to be connected by hydrogen-bonded water filaments. These strong water filaments have been suggested by indirect experiments [8] and results of Monte Carlo simulations [9]. They connect a phosphate group P_n at one side of the major groove with an another phosphate group $P_{n\pm4}$ at the opposite side. Therefore, in order to take into account the presence of this dynamically stable filament, the model must include a coupling between the nth nucleotide on one strand and the $(n+h)$th one on the other ($h=4$ according to the experiments). Such an extension was carried out by Gaeta [10], but he considered only its consequences on the dispersion curves of the small-amplitude excitations of the molecule. We consider here the nonlinear excitations in the extended model and show how the additional coupling increases the ability of the molecule to bear rather broad and sufficiently large-amplitude breatherlike modes, which propagate easily along the molecule.

2. Model

In our model we consider a simplified geometry for the DNA chain, in which we have neglected the asymmetry of the molecule and we represent each strand by a set of point masses which correspond to the nucleotides. The characteristics of the model are the following:

(i) Like Peyrard and Bishop [2], we only take into account transversal motions. The displacement from equilibrium of the nth nucleotide is denoted u_n (v_n)

for the chain C_1 (C_2). The longitudinal displacements are not considered because their typical amplitudes are significantly smaller than the amplitudes of the transversal ones [11].

(ii) Two neighboring nucleotides of the same strand are connected by a harmonic potential because we assume that the displacements due to the bubbles change only gradually from one site to the next. On the other hand, the bonds connecting the two bases belonging to different strands are extremely stretched when the double helix opens locally: their nonlinearity must not be ignored. We use a Morse potential to represent not only the hydrogen bonds but the repulsive interactions of the phosphate and the surrounding solvent action as well.

(iii) Finally, we add to the model introduced by Peyrard and Bishop, a harmonic coupling which takes account of the helical geometry discussed above. It connects the nth mass on the chain C_1 to both the $(n+h)$th and $(n-h)$th masses on chain C_2.

Therefore the Hamiltonian is written as

$$H=\sum_n \left(\tfrac{1}{2}m(\dot{u}_n^2+\dot{v}_n^2)+\tfrac{1}{2}k[(u_n-u_{n-1})^2 + (v_n-v_{n-1})^2]+D\{\exp[-a(u_n-v_n)]-1\}^2 + \tfrac{1}{2}K[(u_n-v_{n+h})^2+(u_n-v_{n-h})^2]\right), \quad (1)$$

where the four terms are respectively the kinetic energy of the transverse vibrations, the potential energy of the longitudinal, transverse (analog to a substrate potential) and helicoidal connections. Here k (K) is the harmonic constant of the longitudinal (helicoidal) spring, m the nucleotide mass and D (a) the depth (width) of the Morse potential.

The dynamical equations deriving from this Hamiltonian are therefore

$$m\ddot{u}_n=k(u_{n+1}+u_{n-1}-2u_n)+K(v_{n+h}+v_{n-h}-2u_n) +2aD\{\exp[-a(u_n-v_n)]-1\} \times\exp[-a(u_n-v_n)], \quad (2)$$

$$m\ddot{v}_n=k(v_{n+1}+v_{n-1}-2v_n)+K(u_{n+h}+u_{n-h}-2v_n) -2aD\{\exp[-a(u_n-v_n)]-1\} \times\exp[-a(u_n-v_n)]. \quad (3)$$

The motions of the two strands can be described in terms of the variables $x_n=(u_n+v_n)/\sqrt{2}$ and $y_n=(u_n-v_n)/\sqrt{2}$ which represent the in-phase and out-of-phase motions respectively. We have then

$$m\ddot{x}_n=k(x_{n+1}+x_{n-1}-2x_n) +K(x_{n+h}+x_{n-h}-2x_n), \quad (4)$$

$$m\ddot{y}_n=k(y_{n+1}+y_{n-1}-2y_n)-K(y_{n+h}+y_{n-h}+2y_n) +2\sqrt{2}\,aD[\exp(-a\sqrt{2}\,y_n)-1] \times\exp(-a\sqrt{2}\,y_n). \quad (5)$$

The two equations decouple exactly. Eq. (4) is a discrete linear equation with the usual plane wave solutions. On the other hand, eq. (5) contains an extra nonlinear term. If one performs an expansion of the Morse potential, keeping only linear terms in eq. (5), we obtain linearized equations whose solutions can easily be obtained assuming they have the form of plane waves with a wave vector $\boldsymbol{q}$ and a frequency ω. We find two dispersion relations, corresponding to an acoustical ($\lim_{|q|\to 0}\omega_a=0$) and an optical branch ($\lim_{|q|\to 0}\omega_o\neq 0$) given explicitly by

$$\omega_a^2=(4/m)[k\sin^2(ql/2)+K\sin^2(qhl/2)], \quad (6)$$

$$\omega_o^2=(4/m)[a^2D+k\sin^2(ql/2) +K\cos^2(qhl/2)], \quad (7)$$

where l is the distance between adjacent nucleotides on the same strand. In the limit $K=0$, these dispersion relations tend to the corresponding ones [6] of the original model without helical coupling, but we

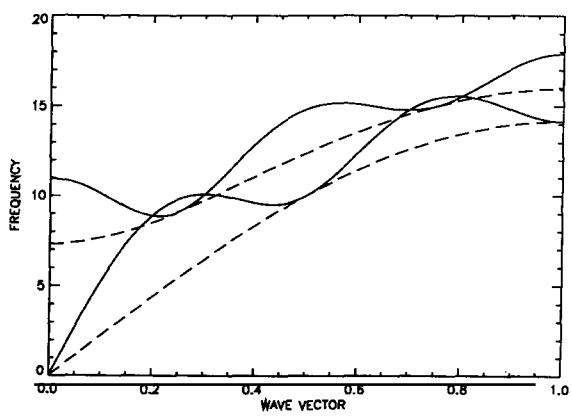

Fig. 1. Acoustical and optical frequency (in ps^{-1}) versus the normalized wave vector, inside the first Brillouin zone. The dashed line corresponds to the model introduced by Peyrard and Bishop, the solid line to our helicoidal model (see the parameter values in the text).

can notice that the introduction of the new coupling affects the spectrum, by increasing the frequencies and introducing oscillations (fig. 1) in agreement with Gaeta's results [10].

3. Breather in the semi-discrete approximation

Let us focus our attention on the nonlinear equation (5), which includes the only degree of freedom interesting for local denaturation: the stretching y_n between two nucleotides of different strands.

We are interested in collective oscillations which are large enough to be strongly anharmonic, but still much smaller than the motions which result in permanently open states; where the nucleotides reach the plateau of the Morse potential. In this hypothesis, the atoms oscillate near the bottom of the potential well, so that we assume $y=\epsilon\phi$ (where $\epsilon \ll 1$) and expand the substrate potential to fourth order terms in $\epsilon\phi$. We obtain

$$V(y)=D[\exp(-a\sqrt{2}\,y)-1]^2$$
$$=2Da^2\epsilon^2\phi^2(1-a\sqrt{2}\,\epsilon\phi+\tfrac{7}{6}a^2\epsilon^2\phi^2)+O((\epsilon\phi)^5)\,,$$

and the equation of motion is

$$\ddot{\phi}_n=\frac{k}{m}(\phi_{n+1}+\phi_{n-1}-2\phi_n)$$
$$-\frac{K}{m}(\phi_{n+h}+\phi_{n-h}+2\phi_n)$$
$$-\omega_g^2(\phi_n+\alpha\phi_n^2\epsilon+\beta\phi_n^3\epsilon^2) \qquad (8)$$

by setting $\omega_g^2=4a^2D/m$, $\alpha=-3a/\sqrt{2}$ and $\beta=\frac{7}{3}a^2$.

According to the experimental results, the problem implies two times-scales:

(i) the first one corresponds to the vibration of the particle around its equilibrium position;

(ii) the second, much larger one, is relative to the propagation of a collective coherent structure along the chain.

So we will use the reductive perturbation method in which we expand in the small parameter ϵ and, using $\theta_n=qnl-\omega t$ (where ω is the optical frequency ω_o of the linear approximation), we substitute

$$\phi_n(t)=\epsilon[F_1(\epsilon nl,\epsilon t)\exp(i\theta_n)+\text{c.c.}]$$
$$+\epsilon^2[F_0(\epsilon nl,\epsilon t)+F_2(\epsilon nl,\epsilon t)\exp(2i\theta_n)+\text{c.c.}]$$
$$+O(\epsilon^3) \qquad (9)$$

in (8) by using the semi-discrete approximation [12] (the complete continuum limit would be too restrictive for DNA, where discreteness effects may be important). Indeed, as we limit ourselves to excitations with large enough width, we can determine the envelope in the continuum limit, as function of the slow variables $Z=\epsilon z$ and $T=\epsilon t$, while the fast oscillations of the quasiharmonic carrier, inside the envelope, are treated exactly. Equating the coefficients of ϵ for each harmonic, we get $F_0=\mu|F_1|^2$ and $F_2=\delta F_1^2$, and finally obtain the nonlinear Schrödinger (NLS) equation for the envelope function F_1,

$$i\frac{\partial F_1}{\partial\tau}+P\frac{\partial^2F_1}{\partial S^2}+Q|F_1|^2F_1=0\,, \qquad (10)$$

where we have made the transformation $\tau=\epsilon T$ and $S=Z-V_gT$, with the linear group velocity

$$V_g=d\omega/dq=l[k\sin(ql)-Kh\sin(qhl)]/m\omega\,,$$

the dispersion coefficient

$$P=\{l^2[k\cos(ql)-Kh^2\cos(qhl)]/m-V_g^2\}/2\omega$$

and the nonlinear one

$$Q=-\omega_g^2[2\alpha(\mu+\delta)+3\beta]/2\omega\,.$$

We will briefly discuss the stability of the analytic solutions of the NLS, which depends on the signs of PQ. However, to simplify this study, we expand these quantities to first order terms in q (a numerical study shows that the results of the stability discussion are almost unaffected by this expansion), since in the next section we limit ourselves to large-width bubbles, i.e. $q \ll 1$.

In this limit, P has the sign of $k-Kh^2$ and Q of $1-\frac{7}{8}K/a^2D$. Therefore the solutions change qualitatively, depending on the value of K. PQ is negative for $k/h^2 \leqslant K \leqslant \frac{8}{7}a^2D$; in this case, the solution of (10) is a finite-amplitude plane wave with a dip near $S-u_e\tau\approx 0$, called a dark-soliton [13] (or an envelope hole), which does not correspond to the small amplitude limit of breather modes. For $0 \leqslant K \leqslant k/h^2$ (this case includes the usual model without helicoidal coupling) and $\frac{8}{7}a^2D \leqslant K$, PQ is positive; we have plane wave solutions, unstable because of modulational (or Benjamin–Feir) instability, and a localised envelope solution, with a vanishing amplitude at $|z|\to\infty$; such a solution has the appropriate shape to represent breathing modes in DNA.

Therefore, the solution of (10) is then [14]

$$F_1(S,\tau)=A\,\mathrm{sech}\left(\frac{1}{L_e}(S-u_e\tau)\right)$$
$$\times\exp\left(\mathrm{i}\frac{u_e}{2P}(S-u_c\tau)\right), \qquad (11)$$

with u_e and u_c the velocities of the envelope and carrier waves, the amplitude $A=\sqrt{(u_e^2-2u_eu_c)/2PQ}$ and the width $L_e=2P/\sqrt{u_e^2-2u_eu_c}$. The envelope soliton, solution of (8), is a plane wave with a frequency corrected for the nonlinearity, an amplitude modulated by a sech-type envelope modified by the second harmonic and the non-oscillating components. It reads

$$y_n(t)=2\epsilon A\,\mathrm{sech}[\epsilon(nl-V_et)/L_e]$$
$$\times(\cos(\Theta nl-\Omega t)+\epsilon A\,\mathrm{sech}[\epsilon(nl-V_et)/L_e]$$
$$\times\{\tfrac{1}{2}\mu+\delta\cos[2(\Theta nl-\Omega t)]\})+\mathrm{O}(\epsilon^3), \qquad (12)$$

with $V_e=V_g+\epsilon u_e$, $\Theta=q+\epsilon u_e/2P$ and $\Omega=\omega+(V_g+u_c\epsilon)\epsilon u_e/2P$.

When $K<k/h^2$, we obtain a very narrow pulse, almost identical to those found in the model without helicoidal interactions [6] (because K approaches 0). On the other hand, when $K>\frac{8}{7}a^2D$, the solution is much broader and has a larger amplitude so that it could provide a better representation of the fluctuational openings of DNA. We have investigated its stability numerically.

4. Numerical results

The lifetime of the solutions determined above is an important parameter, because only long-lived excitations can be detected experimentally. First, we discuss briefly the numerical technique, and then we compare the numerical and theoretical results.

Basically, we perform the simulation by using a continuum breather as an initial condition in the discrete lattice, with the complete Morse potential. Then, we simulate the ensuing propagating of the pulse, solving the Newtonian equations of motion with a fourth order Runge–Kutta method. The timestep Δt is chosen so that the total energy of the system is conserved to a relative accuracy better than 10^{-3}.

The question of the choice of parameters for this model is still a controversial topic, as shown by the debate over these values in the literature [15]. We have chosen a dissociation energy $D=0.1$ eV, $a=2$ Å^{-1}, coupling constants $k=1.5$ eV/Å^2 and $K=0.5$ eV/Å^2, a distance between base pairs $l=3.4$ Å and a mass of 300 m.u. for each nucleotide. To generate the bubbles, we choose a small value for the wave vector ($q=0.01$ Å^{-1}) and therefore the wavelength of the carrier wave is in the range of the envelope width: then the solution is similar to a local opening which oscillates.

As long as the amplitude remains in the region where the Taylor development is justified (typically where y is lower than the Morse potential inflection point), our approximations are valid so that the solution can be expected to be stable. In order to describe the large-amplitude fluctuational openings observed in DNA, we must however consider initial conditions with a larger amplitude.

Fig. 2 shows the motion of a breather with an initial amplitude of 1 Å and a half-width of 18 nucleotides. We can see that, when the motion begins, the amplitude adapts to the real substrate potential. The figure exhibits an amplitude modulation not explained by the calculations performed in the limit of small displacements, i.e. at the bottom of the Morse

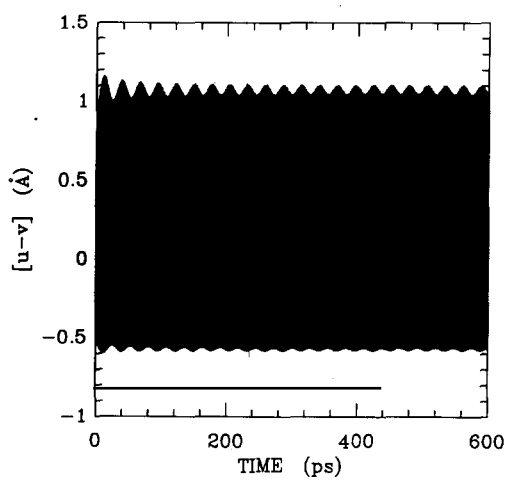

Fig. 2. $u-v$ versus time for the center of the moving breather, followed in his motion. The figure contains about 1000 oscillations of the breather and shows that its amplitude is stable over a very long time ($\epsilon=0.007$, $u_e=10^3$ Å/ps and $u_c=0$ Å/ps). The asymmetry about the $u-v=0$ line is simply a consequence of the asymmetrical potential.

well. Fig. 3 shows these excitations to be very long-lived, although some radiation is emitted by the breather. In spite of this radiation, it should be noticed that the decrease in amplitude is only very weak.

In order to analyse the emitted waves, we plot in fig. 4 the amplitude of the stretching at a distance of 100 particles away from the center of the breather. We can see, after the first burst due to the adaptation, that the radiative rate decreases, and finally corresponds to a permanent emission of resonant phonons, responsible for the instability of the breather. Indeed, a temporal Fourier transform of the same simulation data, started at $t \approx 400$ ps, shows that the frequency of the breathing oscillation $\omega_B = 11.20\,\mathrm{ps}^{-1}$ is about 1% higher than the analytical value; the frequency of the radiated phonons is $\omega_P = 10.97\,\mathrm{ps}^{-1}$, which coincides with ω within 0.2% and attests the coupling mechanism of the breatherlike motion to phonon radiation.

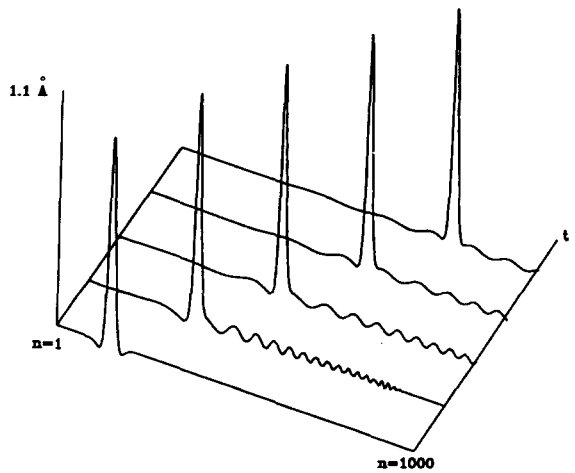

Fig. 3. Propagation of the breather along the chain (only 1000 nucleotides are represented). The period of the breathing oscillation is 0.56 ps and the transverse stretchings are shown every 250 oscillations, when the position of the breather center is at its maximum. Note the asymmetry of the backward and forward radiation patterns.

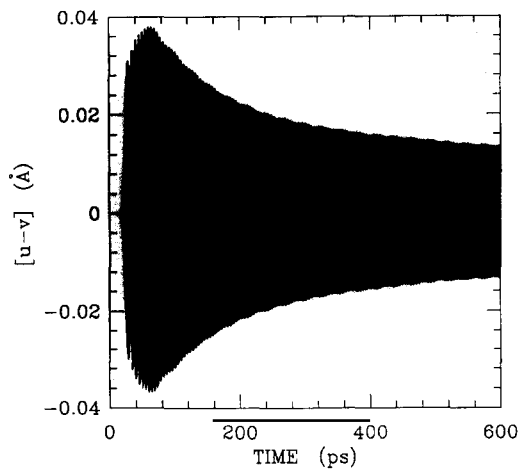

Fig. 4. $u-v$ versus time for a particle at a distance of 100 particles away from the center of the breather. Note that the amplitude is always significantly smaller than the oscillation amplitude of the breather center.

The position of the frequency at the bottom of the dispersion relation ($V_g \approx 0$) explains the slow speed of the radiation packets, compared to the speed of the burst due to adaptation. Besides, the propagation speed of the breather $V_e = 3.7$ Å/ps, is about 20% less than the theoretical value, because of the discreteness effects which usually tend to slow down the motion.

5. Conclusion

In this Letter, our primary aim was to construct a new extended model for the coherent dynamics of bubbles in DNA. We considered, on the one hand, first-neighbor harmonic longitudinal and nonlinear transverse interaction and, on the other hand, an harmonic helicoidal coupling, due to transgroove hydrogen-bonded water filaments. Then envelope solitons, solutions of the NLS equation, were obtained using a perturbation approach and simulation results were used to show the coupling mechanism between the motion of the breather and phonon radiation. Note that the addition of the helicoidal term, introducing modifications in P and Q, has created a special zone without breather modes. We emphasize that this model can have large-amplitude broad oscillations which correspond better to the fluctuational openings of DNA, whereas the previous model with similar parameters cannot.

Finally let us add some remarks. It is known that during the local denaturation, the distance between two nucleotides (in the same strand) undergoes variation [16]. Our model, which includes only transverse motions, cannot take it into account;

however, we can allow the constant K to become a decreasing function of the stretch degree of freedom y. Therefore, with the same method, we can evaluate the upper limit, defining the stability zone of the breather (K_{lim}), which has increased, and it is easy to verify that $\lim_{K \to K\text{lim}} A = \infty$, whereas the width of the opening L_e is invariant. This seems able to give an accurate mechanism for the formation of denaturation bubbles with a very large amplitude.

Nevertheless, it is obvious that before obtaining a suitable description of DNA, we have to take into account the local asymmetry of the two helices, as well as the second principal source of nonlinearity [17] which appears as DNA chains unwind: the bistability of the sugar ring, which allows sugar puckering modes [16].

Acknowledgement

The author would like to thank M. Peyrard for initiating this work and for many helpful comments. He is grateful to H. Hoyet for valuable discussions.

References

[1] M. Karplus and G.A. Petsko, Nature 347 (1990) 631; M. Karplus and J.A. McCammon, Sci. Am. 254 (1986) 30.
[2] M. Peyrard and A. Bishop, Phys. Rev. Lett. 62 (1989) 2755.
[3] M. Peyrard, T. Dauxois and A. Bishop, in: Continuum models and discrete systems, Vol. 2, ed. G.A. Maugin (Longman, London, 1991).
[4] M. Techera, L.L. Daemen and E.W. Prohofsky, Phys. Rev. A 41 (1990) 4543; 42 (1990) 5033.
[5] V. Muto, A.C. Scott and P.L. Christiansen, Phys. Lett. A 136 (1989) 33.
[6] M. Peyrard, in: Proc. Tashkent Workshop, to be published; T. Dauxois and M. Peyrard, in preparation.
[7] E.W. Prohofsky et al., Phys. Lett. A 70 (1979) 492.
[8] U. Dahlborg and A. Rupprecht, Biopolymers 10 (1971) 849.
[9] G. Corongiu and E. Clementi, Biopolymers 20 (1981) 551.
[10] G. Gaeta, Phys. Lett. A 143 (1990) 227.
[11] J.A. McCammon and S.C. Harvey, in: Dynamics of proteins and nucleic acids (Cambridge Univ. Press, Cambridge, 1988).
[12] M. Remoissenet, Phys. Rev. B 33 (1986) 2386.
[13] K. Muroya, N. Saitoh and S. Watanabe, J. Phys. Soc. Japan 51 (1982) 1024.
[14] A. Scott, F. Chu and D.W. McLaughlin, Proc. IEEE 61 (1973) 1443.
[15] L.L. van Zandt, Phys. Rev. A 40 (1989) 6134; 42 (1990) 5036, and references therein; M. Techera, L.L. Daemen and E.W. Prohofsky, Phys. Rev. A 42 (1990) 5033.
[16] W. Saenger, in: Principles of nucleic acid structure (Springer, Berlin, 1984).
[17] H. Sobell, Proc. Natl. Acad. Sci. 82 (1985) 5328.